Advances in Manufacturing Technology XXXV
M. Shafik and K. Case (Eds.)

doi:10.3233/ATDE220583

Stiffness Measurement of Parallel Kinematic Machines Considering Gravity Effect

Shakya BANDARA[a,b,1], Yan JIN[a,2], Mien VAN[a]
Dan SUN[a], Rao FU[c], Patrick CURLEY[a], Colm HIGGINS[a]
[a] *Queen's University Belfast, University Road, Belfast BT7 1NN, UK.*
[b] *Department of Applied Computing, University of Kelaniya, Sri Lanka.*
[c] *Dalian University of Technology, Liaoning Province, PR China.*

Abstract. Parallel Kinematic Machine (PKM) is a new type of machine tool, which has the potential to fill in the gap between traditional CNC machines and industrial robots, due to its flexibility and superior motion dynamics. Stiffness is an essential property of a machine tool, as it will affect the machining capability. Although much research has been conducted on stiffness modelling and analysis, most of them employ simplified models and gravity effects have not been well considered or characterized for PKMs. To fill in the knowledge gap, this paper introduces a new experimental stiffness measurement method considering the effect of gravity on the machine tool. An experimental procedure was developed in order to separate the gravity effects on stiffness from the machine structure.

Keywords. PKM, stiffness, gravity.

1. Introduction

Parallel Kinematic Machine (PKM), also known as parallel robot, is a relatively new type of machine tool compared to traditional numerical control machines (TNCMs). They have been identified as a major contributor to future manufacturing systems because they have flexibility as a serial robot, superior dynamic performance as CNCs, and demonstrate high stiffness to mass ratio [1]. Since the first PKM was introduced to public at the IMTS fair in 1994, research to improve the performances of PKMs has grown exponentially in the past two decades and commercialized PKMs (e.g., Tricept [2], Exechon [3], and A3 Sprint head [4]) have been widely adopted in the industry today [1]. With their high dynamic performances, they have demonstrated the required flexibility and improved precision capability in machining large parts such as drilling and milling of aircraft structures.

Stiffness property is one of the key performance measures of productive machines. Given the closed-loop structure and configuration dependent characteristics, accurate stiffness modelling of PKMs can be very challenging. In literature, the stiffness modelling methods for PKMs can be categorized into three main approaches, namely,

[1] Corresponding Author. vadhikarivitharana01@qub.ac.uk
[2] Corresponding Author. y.jin@qub.ac.uk

(I) numerical approach with FEA [5], [6], (II) analytical approach based on structural matrix [7], [8] , and (III) semi-analytical method based on virtual works principle [9], [10]. In order to reduce complexity, most studies on stiffness modelling focused on the machine structure but neglected the effect of gravity by assuming that the links of the robot are weightless and the joints are perfectly rigid. However, to reflect the reality and increase accuracy, it is essential to consider the gravity effect for stiffness characterization. Lian et al. [11] developed a new 5-DOF PKM named T5 for high-precision machining in aerospace manufacturing and the machine's performance was validated by experiments. Ibaraki et al. [12] proposed a gravity-induced error compensation method for hexapod-type PKMs. Cao et al. [13] presented a stiffness model for an over-constrained parallel mechanism considering the gravity of all moving components and external payloads. Wang et al. [14] proposed a semi-analytical stiffness model for the 3-SPR parallel mechanism. Furthermore, gravity-induced error compensation methods for serial industrial robot manipulators have been discussed in [15] and [16]. Apart from that, few other studies found in the literature [17]–[19] describe the effect of the gravity on serial and parallel manipulators, stiffness modelling and gravity error compensation methods. Although these methods have accounted gravity effects via theoretical approaches, there is no study yet to directly measure the gravity effects on PKM stiffness through experiments. Direct measurement will give more accurate results compared to the theoretical estimations. These experimental results utilized for optimizing these hard-to-measure parameters (e.g., compliance of a gimbal) used in stiffness modelling. To address these issues, this paper will investigate the gravity effect directly through stiffness experiments with Exechon X-mini PKM. The rest of the paper is organized as follows. Section 2 shows the gravity effect analysis, and section 3 introduces the experimental procedure for stiffness measurement in X-mini PKM.

2. Gravity effect analysis and theoretical model of stiffness measurement

To obtain the machine stiffness considering the gravity, the procedure given below was followed. Care should be taken that gravity is continuously exerted on the machine tool at any configuration, and the PKM's stiffness will be configuration dependent. The experimental procedure was developed in order to separate the gravity effects on stiffness from the machine tool structure.

As shown in Figure 1. (A), a reference coordinate system $\{O\text{-}x_o y_o z_o\}$ was defined at the middle position of the axis which passes through the leg 1 and leg 3 base joint axis, and the gravity is acting in the y_o-direction. During the experiment, the exerted forces were applied in either positive or negative y_o-direction. Two methods were used to measure the machine tool displacement under the applied forces via a force adaptor. First, force F_1 was applied, where the direction of force was from tombstone to tooltip in the upward direction (i.e. - y_o), as shown in Figure 1. (B) In the next attempt, force F_2 was applied by hanging weights on the tooltip where the direction of applied force was from tool tip to downward direction (i.e. + y_o), as shown in Figure 1. (C).

The diagram in Figure 2 shows four different positions of the tooltip under the applied loads. Figure 2. (A) shows the ideal position of the tooltip without the gravity effect. Figure 2. (B) shows the initial position of the tooltip under gravity without external forces. Displacement of the tooltip due to gravity is considered as δy_g as shown in Figure 2. (B). Figure 2. (C) shows the position tooltip under the applied force from

bottom to upward direction. Displacement of the tooltip due to upward force is δy_1. Figure 2. (D) shows the position tooltip under the applied force from up to downward direction. Displacement of the tooltip due to downward force is δy_2.

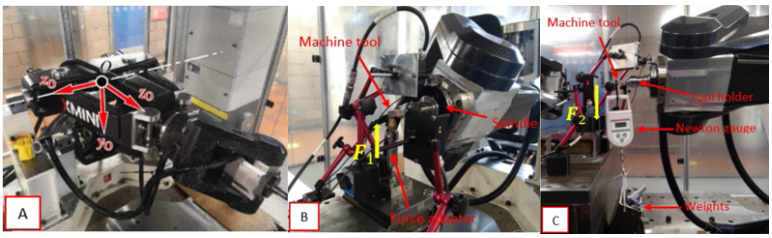

Figure 1. (A): Pose of the reference coordinate system, (B): Experimental setup to measure the displacement in Y direction upward, (C): Experimental setup to measure the displacement in Y direction downwards.

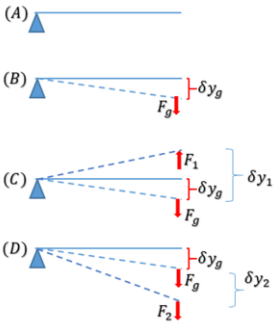

Figure 2. Different positions of the tooltip under applied forces. (A): home position of the whole machine without gravity and external load, (B): deformation at tooltip with gravity only, (C): deformation at tooltip with both gravity and external load upward (opposite to the direction of gravity), (D): deformation at tooltip with both gravity and external load.

Considering each position of the tooltip, the following equations can be obtained by applying Hooke's law. From Figure 2. (B), considering the initial position of the tooltip with the gravity,

$$Fg = K_g \delta y_g, \tag{1}$$

where Fg is the force due to gravity and K_g is the stiffness at the initial tool position and the variations of K_g are assumed to be negligible during the micro-deformation. From Figure 2. (C), considering the resultant force in the downward direction,

$$Fg - F_1 = K_1 \delta y_1, \tag{2}$$

where F_1 is the applied force in the upward direction, and K_1 is the stiffness of the machine related to the position in Figure 2. (C). From Figure 2. (D), considering the resultant forces in the downward direction,

$$Fg + F_2 = K_2(\delta y_g + \delta y_2), \tag{3}$$

where F_2 is the applied force in the downward direction, and K_2 is the stiffness of the machine related to the position in Figure 2. (D). Since δy_i *(i=1,2, g)* is very small, assume the stiffnesses at each point are equal, i.e., $K_1 = K_2 = K_g = K$, then, the following equation is obtained from Eqn. (1) and Eqn. (3).

$$K = \frac{F_2}{\delta y_2}, \tag{4}$$

Using Eqn. (4) and experimental data, the stiffness of the machine tool K for the relevant coordinates were obtained.

3. Experimental setup and procedure

3.1. Experimental Setup

To measure the displacement of the spindle and tool under the applied static load, two laser displacement sensors (LDS) and two eddy current displacement (ECS) sensors were used, as shown in Figures 3. (A) and Figure 3. (B). The two LDS were used to measure the tool displacement in X and Y directions as shown in Figure 3. (A). Eddy current sensors were used to measure the tool displacement along Z-axis and the displacement of spindle along Y-axis as shown in Figure 3. (B).

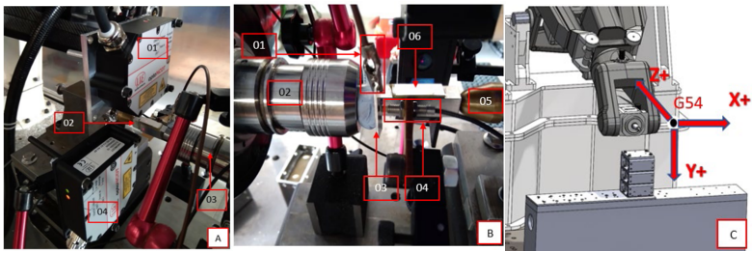

Figure 3. (A)- LDS setup to measure the tool displacement in X and Y directions (1: LDS1, 2: Cutting tool, 3: Tool holder, 4: LDS2). (B)- ECS setup to measure the displacement in the Z direction (1: Ground cable, 2: Tool holder, 3: ECS target plate, 4: ECS, 5: Force sensor tip, 6: Cutting tool). (C)- Orientation of the G54 coordinate system.

3.2. Procedure

G54 machine coordinate system was used to measure the displacement of the tool under the applied load. G54 coordinate system showed in Figure 2. (C) is related to the reference coordinate system O as G54 (0, 0, 0) = O (-6.493, 268.780, 1420.431). To apply the load on the tooltip in upward direction, pre-designed fixture blocks and a force adaptor were used as shown in Figure 1. (B). First, the fixture blocks and the force adaptor are mounted on the tombstone. Then, the sensors were mounted and aligned accordingly before starting the experiment. After setting up the sensors, the initial sensor readings were recorded. Next, the load was applied using the force adaptor until the force sensor reading was around 100N. After that, the sensor readings were re-recorded. To measure the displacement under the applied force in the downward direction, a newton gauge was fixed at the tooltip and weights were applied until the newton gauge gave around 100N reading, as shown in Figure 1. (C). Displacements of the tooltip was recorded using the same sensor setup as the previous case. The same procedure was repeated to record the tool displacement in different coordinates of the workspace.

4. Results

The stiffness values in Y direction (Ky) in ten different positions of the workspace were calculated using Eqn. (4) as described in section 2. The calculated stiffness values, related coordinates and applied forces in upward and downward directions are presented in Table 1. Using Eqn. (1) and Eqn. (2), the gravity force (Fg) acting on each position and the gravity-related tool deflection (δy_g) were calculated. These values

(Ky, $Fg, \delta y_g$) represent the dependency of stiffness and the effect of gravity with different positions in the workspace. It is clear from the data that the gravity force acting on the tooltip is much higher than the applied external force, for example during the experiment, the applied external force is around 100N, but the calculated gravity force in same coordinate always higher than 200N. As a result, the gravity force may create higher deflections in the tooltip than the cutting force for small cutting forces. Therefore, considering the effect of gravity in stiffness modelling is essential to increase the accuracy of the model.

Table 1. Experimental data and calculated stiffness in the Y direction.

Coordinates			Force (N)		$\delta y1$ (µm)	$\delta y2$ (µm)	Ky (N/mm)	Fg (N)	δyg (µm)
X	Y	Z	F1	F2					
-395.81	271.03	1286.36	100.5	100.6	136.53	122.98	818.05	212.19	259.38
-244.48	344.93	1359.81	100.5	100.4	126.33	101.31	991.00	225.69	227.74
-217.08	-40.99	1437.58	100.3	100.4	158.99	105.37	952.85	251.79	264.25
-82.09	-41.27	1437.26	100.5	100.2	148.26	116.20	862.34	228.35	264.81
11.37	269.39	1360.39	100.4	100.2	134.60	104.86	955.55	229.02	239.67
28.52	344.37	1359.16	100.6	100.2	136.40	96.72	1036.02	241.92	233.51
52.92	-41.54	1436.94	100.3	100.4	133.50	112.74	890.58	219.19	246.12
188.91	-41.82	1436.62	100.4	100.4	155.13	106.72	940.81	246.35	261.85
333.37	268.74	1359.63	100.4	100.6	136.64	101.83	987.96	235.40	238.26
467.36	268.46	1359.32	100.4	100.6	172.34	105.62	952.46	264.55	277.75

5. Conclusion

In this study, a novel stiffness measurement method was proposed for PKM machine tools, which can separate the effect of gravity on machine tool components from stiffness. Experiments were conducted on the Exechon X-mini PKM and the stiffness of the machine tool in different coordinates was calculated eliminating the effect of gravity. The method is entirely based on an experimental procedure and can be used with the PKM machine tool. For future work, the research group is developing a complete stiffness model for PKM to predict the stiffness of the whole workspace considering the effect of gravity. The data obtained from this study will be used to calibrate the model parameters of a theoretical stiffness model to predict the stiffness of the machine tool considering the effect of gravity.

Acknowledgements

The funding support from EPSRC projects EP/P025447/1 and EP/P026087/1 is acknowledged. This project has also received funding from the European Union's Horizon 2020 research and innovation program under grant agreement No 734272. This work was supported by Larmor University Studentship 2021 from Queen's University

Belfast and the Accelerating Higher Education Expansions and Development (AHEAD) Operation fund by the World Bank in Sri Lanka.

References

[1] M. Weck and D. Staimer, "Parallel kinematic machine tools - Current state and future potentials," *CIRP Ann. - Manuf. Technol.*, vol. 51, no. 2, pp. 671–683, Jan. 2002, doi: 10.1016/S0007-8506(07)61706-5.

[2] K.-E. Neumann, "Robot," US Patent 4732525, Apr. 21, 1988.

[3] K.-E. Neumann, "Parallel-Kinematical Machine," US Patent 8783127, 2014.

[4] Y. Ni, B. Zhang, Y. Sun, and Y. Zhang, "Accuracy analysis and design of A3 parallel spindle head," *Chinese J. Mech. Eng.*, vol. 29, no. 2, pp. 239–249, Mar. 2016, doi: 10.3901/CJME.2015.1210.144.

[5] A. Pashkevich, D. Chablat, and P. Wenger, "Stiffness analysis of overconstrained parallel manipulators," *Mech. Mach. Theory*, vol. 44, no. 5, pp. 966–982, May 2009, doi: 10.1016/J.MECHMACHTHEORY.2008.05.017.

[6] A. Klimchik, D. Chablat, and A. Pashkevich, "Stiffness modeling for perfect and non-perfect parallel manipulators under internal and external loadings," *Mech. Mach. Theory*, vol. 79, pp. 1–28, Sep. 2014, doi: 10.1016/j.mechmachtheory.2014.04.002.

[7] D. Deblaise, X. Hernot, and P. Maurine, "A systematic analytical method for PKM stiffness matrix calculation," *Proc. - IEEE Int. Conf. Robot. Autom.*, vol. 2006, pp. 4213–4219, 2006, doi: 10.1109/ROBOT.2006.1642350.

[8] J. Wu, J. Wang, L. Wang, T. Li, and Z. You, "Study on the stiffness of a 5-DOF hybrid machine tool with actuation redundancy," *Mech. Mach. Theory*, vol. 44, no. 2, pp. 289–305, Feb. 2009, doi: 10.1016/J.MECHMACHTHEORY.2008.10.001.

[9] A. Klimchik, A. Pashkevich, and D. Chablat, "CAD-based approach for identification of elasto-static parameters of robotic manipulators," *Finite Elem. Anal. Des.*, vol. 75, pp. 19–30, Nov. 2013, doi: 10.1016/J.FINEL.2013.06.008.

[10] P. C. López-Custodio, R. Fu, J. S. Dai, and Y. Jin, "Compliance model of Exechon manipulators with an offset wrist," *Mech. Mach. Theory*, vol. 167, no. October 2021, p. 104558, Jan. 2022, doi: 10.1016/j.mechmachtheory.2021.104558.

[11] B. Lian, T. Sun, Y. Song, Y. Jin, and M. Price, "Stiffness analysis and experiment of a novel 5-DoF parallel kinematic machine considering gravitational effects," *Int. J. Mach. Tools Manuf.*, vol. 95, pp. 82–96, Aug. 2015, doi: 10.1016/j.ijmachtools.2015.04.012.

[12] M. Nakagawa, T. Matsushita, T. Ando, Y. Kakino, S. Ibaraki, and H. Takaoka, "Compensation of Gravity-induced Errors on Hexapod-type Parallel Mechanism Machine Tools," *Proc. Int. Conf. Lead. Edge Manuf. 21st century LEM21*, vol. 2003, no. 0, pp. 619–624, 2003, doi: 10.1299/jsmelem.2003.619.

[13] W. Cao, H. Ding, and W. Zhu, "Stiffness modeling of overconstrained parallel mechanisms under considering gravity and external payloads," *Mech. Mach. Theory*, vol. 135, pp. 1–16, May 2019, doi: 10.1016/j.mechmachtheory.2018.12.031.

[14] M. Wang, H. Liu, T. Huang, and D. G. Chetwynd, "Compliance analysis of a 3-SPR parallel mechanism with consideration of gravity," *Mech. Mach. Theory*, vol. 84, pp. 99–112, Feb. 2015, doi: 10.1016/j.mechmachtheory.2014.10.002.

[15] P. Xu *et al.*, "Stiffness modeling of an industrial robot with a gravity compensator considering link weights," *Mech. Mach. Theory*, vol. 161, p. 104331, Jul. 2021, doi: 10.1016/j.mechmachtheory.2021.104331.

[16] A. Klimchik, S. Caro, Y. Wu, D. Chablat, B. Furet, and A. Pashkevich, "Stiffness Modeling of Robotic Manipulator with Gravity Compensator," in *Mechanisms and Machine Science*, vol. 15, no. May, 2014, pp. 185–192.

[17] J. Fan, H. Tao, R. Pan, and D. Chen, "Optimal tolerance allocation for five-axis machine tools in consideration of deformation caused by gravity," *Int. J. Adv. Manuf. Technol.*, vol. 111, no. 1–2, pp. 13–24, 2020, doi: 10.1007/s00170-020-06096-x.

[18] A. Klimchik, A. Pashkevich, D. Chablat, and G. Hovland, "Compliance error compensation technique for parallel robots composed of non-perfect serial chains," *Robot. Comput. Integr. Manuf.*, vol. 29, no. 2, pp. 385–393, Apr. 2013, doi: 10.1016/j.rcim.2012.09.008.

[19] L. Nguyen Vu and C. H. Kuo, "An analytical stiffness method for spring-articulated planar serial or quasi-serial manipulators under gravity and an arbitrary load," *Mech. Mach. Theory*, vol. 137, pp. 108–126, Jul. 2019, doi: 10.1016/j.mechmachtheory.2019.03.015.